sustainability

MDPI

Article

Valorization of Recycled Aggregate and Copper Slag for Sustainable Concrete Mixtures: Mechanical, Physical, and Environmental Performance

Pamela Wendy Caballero Arredondo [1], Yimmy Fernando Silva [1,2,3,*], Gerardo Araya-Letelier [1,2] and Héctor Hernández [1]

[1] School of Civil Construction, Faculty of Engineering, Pontificia Universidad Católica de Chile, Santiago 7820680, Chile; pecaballero@uc.cl (P.W.C.A.); gerardo.araya@uc.cl (G.A.-L.); hehernan@uc.cl (H.H.)
[2] Concrete Innovation Hub UC (CIHUC), Faculty of Engineering, Pontificia Universidad Católica de Chile, Santiago 7820680, Chile
[3] Composite Materials Group (CENM), Universidad del Valle, Cali 760042, Colombia
* Correspondence: yimmy.silva@uc.cl

Abstract: The increasing environmental impacts caused by the high demand for concrete production have underscored the need for sustainable alternatives in the design of eco-concrete mixtures. Additionally, important industries, such as construction and mining, generate massive amounts of waste/by-products that could be repurposed towards sustainability. Consequently, this study investigates the valorization of copper slag (CS), a by-product of the mining industry as a supplementary cementitious material (SCM), and concrete as recycled coarse aggregate (RCA), derived from construction and demolition waste, as partial substitutes for Ordinary Portland Cement (OPC) and natural coarse aggregate (NCA), respectively. Eco-concrete mixtures were designed with varying replacement levels: 15% for CS, and 0%, 20%, 50%, and 100% for RCA. The mechanical properties (compressive, indirect tensile, and flexural strengths), permeability characteristics (porosity and capillary suction), and environmental impacts (carbon footprint) of these mixtures were evaluated. The results showed that the use of CS and of increasing proportions of RCA led to a monotonic loss in each of the concretes' mechanical strength properties at 7, 28 and 90 days of curing. However, at extended ages (180 days of curing), the concrete mixtures with CS and only NCA presented an average compressive strength 1.2% higher than that of the reference concrete (mixture with only OPC and natural aggregate). Additionally, the concrete mixture with CS and 20% RCA achieved 3.2% and 5.8% higher average values than the reference concrete in terms of its indirect tensile strength and flexural strength, respectively. Finally, a cradle-to-gate life cycle assessment (LCA) analysis was implemented, whose results showed that the greatest effect on reducing the carbon emission impacts occurred due to the substitution of OPC with CS, which confirmed that the adequate technical performances of some of the concrete mixtures developed in this study are positively complemented with reduced environmental impacts. Moreover, this study presents a viable approach to minimizing resource consumption and waste generation, contributing to the advancement of eco-friendly construction materials, which aligns with the sustainable development goals.

Keywords: eco-concrete; waste valorization; copper slag; recycled coarse aggregate; environmental impacts

check for updates

Citation: Arredondo, P.W.C.; Silva, Y.F.; Araya-Letelier, G.; Hernández, H. Valorization of Recycled Aggregate and Copper Slag for Sustainable Concrete Mixtures: Mechanical, Physical, and Environmental Performance. *Sustainability* **2024**, *16*, 11239. https://doi.org/10.3390/su162411239

Academic Editor: Paulo Santos

Received: 19 November 2024
Revised: 10 December 2024
Accepted: 17 December 2024
Published: 21 December 2024

Copyright: © 2024 by the authors. Licensee MDPI, Basel, Switzerland. This article is an open access article distributed under the terms and conditions of the Creative Commons Attribution (CC BY) license (https://creativecommons.org/licenses/by/4.0/).

1. Introduction

Concrete is the most widely used manufactured material in the construction of housing and infrastructure [1,2] due to its advantages, including durability, strength, cost effectiveness, local availability, and constructability [3–5]. However, its high embodied energy, as well as its high demand, have caused severe environmental problems, due to the generation of carbon dioxide (CO_2), large-scale mining of natural aggregate, and accumulation of

construction and demolition waste, among other issues [6,7]. For example, the construction industry was responsible for the emission of 11.7 gigatonnes of CO_2, equivalent to 37% of the global total, in 2020 [8]; of this, approximately 8% was generated by cement production [9], due to the high consumption of this binder, which reaches approximately 4.2 billion tons annually. Additionally, nearly 40 billion tons of aggregates (both fine and coarse) are used annually for concrete production [10,11]. To mitigate the environmental impacts generated by the construction industry, researchers and industry practitioners have proposed different strategies to reduce the negative effects linked to concrete manufacturing [12–14]. In the field of concrete technology, various promising alternatives have arisen, including, but not limited to, the following: (i) the use of recycled aggregate as a replacement for natural aggregate [15,16]; and (ii) the use of supplementary cementitious materials (SCMs) as a partial replacement for cement, such as coconut shell ash, calcined clay, masonry residue, copper slag (CS), sugarcane bagasse ash, ground granulated blast furnace slag (GGBFS), and fly ash (FA), which have been shown to improve compressive, flexural, and durability characteristics [17–24].

The use of SCMs such as FA [25], GGBFS [1], silica fume [26], and metakaolin (MK) [27] in cement-based materials (i.e., cement pastes, mortar, and concrete mixtures) as partial replacements offers several advantages, such as improved mechanical performance and long-term durability. At the same time, in the search for sustainable alternatives to traditional SCMs, and in response to the high volume of CS generated by copper industries, the valorization of this waste/by-product is becoming increasingly attractive [19,28,29]. CS is a waste/by-product of pure copper refining and smelting [30]. Worldwide, about 68.8 million tons of CS are generated annually [31], and this high amount is due to the fact that for each ton of copper metal produced, 2.2 to 3 tons of CS are generated [3,32]. In detail, CS consists of several oxides, such as iron oxide (Fe_2O_3), silica (SiO_2), alumina (Al_2O_3), limestone (CaO), magnesium oxide (MgO), and other metals in smaller quantities [33,34]. The composition of CS depends on the smelting method. The use of CS as an alternative SCM to those previously mentioned has shown initial promising benefits in the production of new concrete mixtures, such as a decrease in the release of heat accumulated during hydration, the improvement of flowability, and a reduction in absorption and permeability [3,35]. For instance, the lower accumulated heat release during hydration (when compared to other SCMs, such as silica fume) is evidence of a reduction in the mechanical performance at short ages exhibited by concrete mixtures with CS. However, this effect could be mitigated by further reducing its particle size to increase its surface area (enhancing the activation of CS) and performing rapid cooling upon generation. CS specifically delays the setting of the paste by maintaining the same water content in the mixture (this was determined in this same CS in a parallel study carried out by isothermal calorimetry).

An interesting example of the use of CS in cement-based materials is a study by Gopalakrishnan and Nithiyanantham [36], which evaluated the use of CS as SCM in mortar mixtures. The authors stated that the incorporation of CS (30 wt% replacing of ordinary Portland cement (OPC)) improved compressive strength and significantly reduced porosity after 28 days of curing, with an 11% increase in mechanical strength and a 50% decrease in porosity compared to a reference mixture (100% OPC). However, some studies have reported another behavior in relation to mechanical performance, with a negative effect observed when incorporating CS into concrete mixtures at an early age. For example, Mirhosseini et al. [37] used different percentages of CS (from 20 to 40 wt%) in concrete mixtures, finding a loss of strength in all the mixtures with CS. The losses exceeded 25% when compared to a reference mixture without CS.

On a related note, the use of recycled aggregate from concrete construction and demolition waste (CDW) as a partial or full replacement for natural aggregates provides a viable solution for reducing the demand for virgin materials and carbon emissions while also minimizing the need to dispose of CDW in landfills [38–40]. Since aggregates constitute between 60% and 70% of concrete mixtures, this creates a demand of several billion tons of aggregates annually. For instance, in China, 17.89 billion tons of aggregates were used

in the production of concrete in 2021 [41]. Nevertheless, recycled coarse aggregate (RCA) from CDW, unlike natural coarse aggregate (NCA), is characterized by adhered mortar, which leads to higher absorption, lower density, greater porosity, an unsatisfactory crushing index, and the presence of an interfacial transition zone (ITZ) [7,15,42]. The quality of RCA determines its application; high-quality RCA is suitable for structural concrete, whereas low-quality RCA is limited to non-structural concrete or use in roadbed fill. Among the factors influencing RCA quality, Xia and Zhao [43] investigated the effect of the ITZ and the old mortar adhered to RCA by preparing concrete mixtures with different water-to-cement ratios (0.4, 0.5, and 0.6) and mortar contents. It was found that the recycled aggregates from concrete with a lower water-to-cement ratio presented enhanced compressive strength performance. In response to the current need to develop more sustainable concrete mixtures and explore alternative materials with reduced environmental impacts, this research analyzed the dual effect of using CS as SCM and recycled aggregate from CDW as a coarse aggregate in the design of new concrete mixtures, an area that remains underexplored in both the short and long term. To the best of the authors' knowledge, this is the first study evaluating the combined effect of CS and RCA in the mechanical/durability and environmental performance of concrete mixtures in both the short and long term. Moreover, this study also provides a comprehensive understanding of the benefits and disadvantages of the combined use of this by-product and CDW. Consequently, the objective of this work is to assess the combined effects of increasing the dosages of CS (0% and 15% vol. replacement of OPC) and RCA (0%, 20%, 50%, and 100% vol. replacement of NCA) in concrete mixtures (including a control mixture with only OPC and 100% NCA), evaluating the following features: (i) workability (slump); (ii) mechanical properties in the short and long term (i.e., compressive strength, flexural strength, and indirect tensile strength); (iii)permeability properties in the short and long term (i.e., absorption and capillary suction); and (iv) environmental impacts (i.e., amount of CO_2 generated in each of the concrete mixtures). To achieve the above-mentioned objectives, this paper is organized as follows: Section 2 describes the concrete constituent materials, the design mixtures, the experimental methods, and the carbon footprint assessment methodology employed in this study. Detailed results and a discussion are provided in Section 3. Finally, Section 4 presents the main conclusions and future work recommendations of this study.

2. Materials and Methods

In this study, OPC type I, according to ASTM C150 [44], was utilized as a cementitious binder. The CS used as SCM was obtained from the Codelco company, located in Valparaíso, Chile the world's largest copper producer [45]. The chemical composition, determined using an X-ray fluorescence spectrometer (XRF), and the morphology of the particles of OPC and CS are presented in Table 1 and Figure 1, respectively. It can be observed that the main oxides of the CS are Fe_2O_3, SiO_2, and Al_2O_3, and the morphology of this waste/by-product after milling corresponds to irregular and angular particles. Similarly, the OPC exhibits comparable morphological characteristics, including an irregular shape and a range of particle sizes.

Table 1. Chemical composition of CS and OPC.

Chemical Composition	CS	OPC
Fe_2O_3	59.15	3.42
SiO_2	29.15	25.08
CaO	2.84	59.15
Al_2O_3	5.84	5.12
CuO	1.34	-
SO_3	1.15	2.73
K_2O	1.28	0.77
TiO_2	0.48	0.28

Table 1. *Cont.*

Chemical Composition	CS	OPC
Na_2O	1.02	0.13
PbO	0.20	-
LOI *	−5.16	1.99

* LOI: lost on ignition.

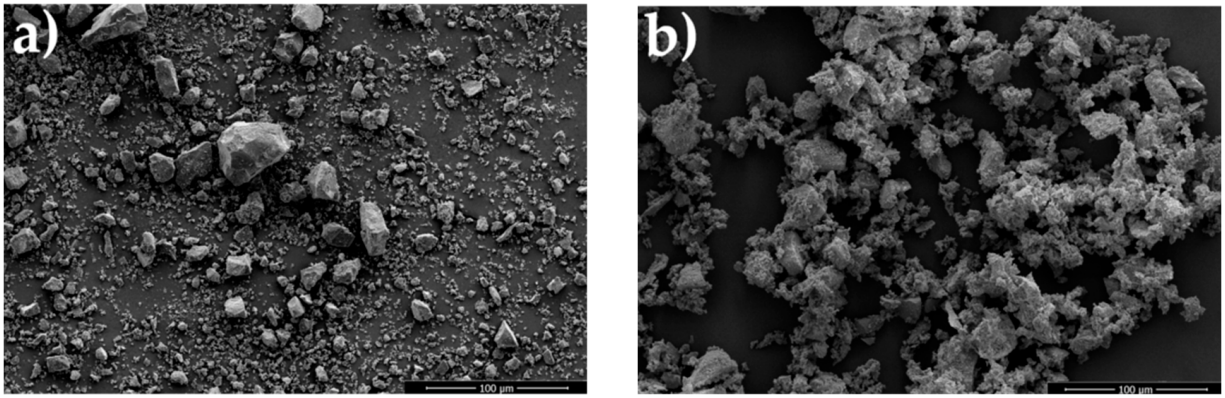

Figure 1. SEM micrographs at 1000× magnification of (**a**) CS and (**b**) OPC.

Figure 2 shows the particle size distribution of OPC and CS, as determined by laser diffraction. The median particle sizes of OPC and CS were 26.48 µm and 17.37 µm, respectively. This is further illustrated in Figure 2, where a significant percentage of larger particles can be observed in the granulometry of the CS (red line).

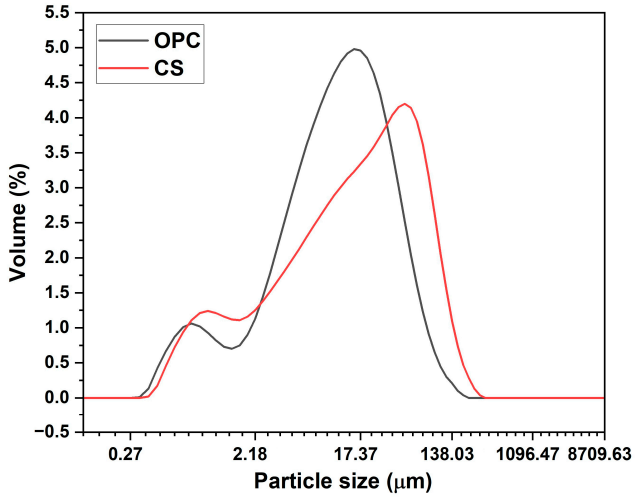

Figure 2. Particle size distribution of OPC and CS.

Another technique used to characterize the pozzolanic activity of CS through the quantification of portlandite (CH) was thermogravimetric analysis (TGA). The first derivatives of the thermogravimetric curves (DTG curves) were used to determine the decomposition temperature ranges of the reaction products formed. Powder samples (reference: paste with 100% OPC; and 20% CS: paste with 80% OPC–20% CS) were analyzed at a heating rate of 10 °C/min in a temperature range of 30 to 1000 °C and a nitrogen atmosphere (it is important to note that typically, the pozzolanic properties of SCMs are evaluated using

a 20% replacement of cement [46,47]; however, other proportions can also be used). The percentage of fixed lime (CH (%)) was estimated according to Equation (1) [48].

$$\text{Fixed CH (\%)} = \frac{(\text{CHc} \times \text{C\%}) - \text{CHp}}{\text{CHc} \times \text{C\%}} \quad (1)$$

where

CHc: amount of CH in the control paste for a given curing time,

CHp: amount of CH in the pozzolan paste at the same age,

C%: proportion of cement in the paste.

Figure 3 illustrates three distinct peaks: (i) the first peak, attributed to the evaporation of free water and the dehydration of C-S-H and C-A-S-H gels and ettringite (E); (ii) the second peak, corresponding to the dehydration of CH (the peak of interest for the calculation of fixed lime (%)); and (iii) the third peak, corresponding to the results from the decarbonation of $CaCO_3$. The amount of CH at 28 days of curing for the reference and 20% CS mixtures was 12.47 and 9.61, respectively, which is equivalent to a CH fixation of 3.33%. This low fixation value indicates a limited pozzolanic performance of CS at early ages [49].

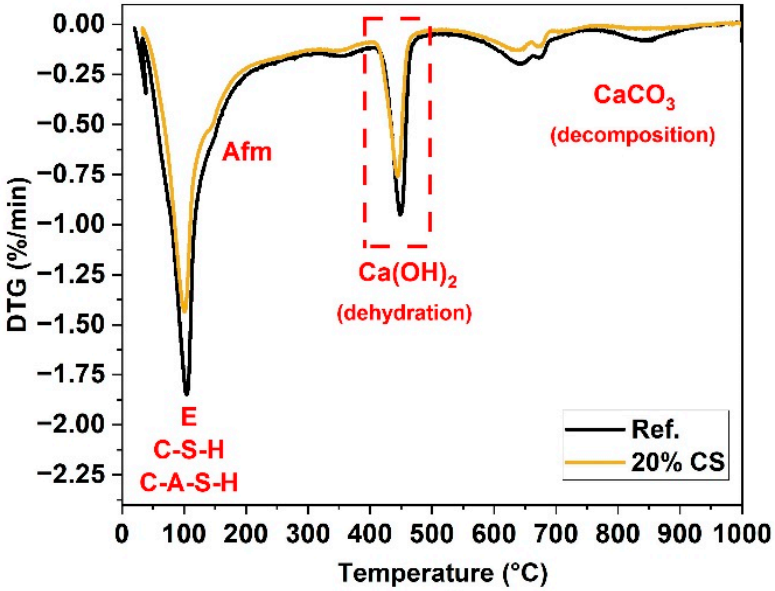

Figure 3. DTG curves of pastes 100% OPC (Ref.) and 80% OPC–20% CS (20% CS).

Local aggregates were utilized for the manufacture of the concrete mixtures. The natural fine aggregate (NFA) consisted of natural medium river sand with a fineness modulus of 2.58, a bulk density of 2590 kg/m^3, and a water absorption rate of 1.62%. The NCA was crushed gravel with a maximum nominal size of 12.5 mm, and the RCA originated from the demolition of concrete structural elements of a 40-year-old building in Santiago, Chile (Figure 4). These elements exhibited a strength of 38 ± 2,1 MPa, as measured via concrete core tests. The particle gradations of the NFA, NCA, and RCA, and the physical properties of the coarse aggregate, are shown in Figure 5 and Table 2. It is worth mentioning that the ITZ of the RCA was not characterized, but the medium-to-low quality of the RCA could be observed by the result of high fragmentation resistance obtained using the Los Angeles abrasion test (27.98), which was approximately twice as high as the value obtained for the NCA (14.43). Furthermore, a superplasticizer (SP) of the polycarboxylate retarding type, with a water-reducing ratio of 30–40% and density of 1050 kg/m^3, was incorporated in this study.



Figure 4. Concrete wastes that were crushed to produce the RCA.

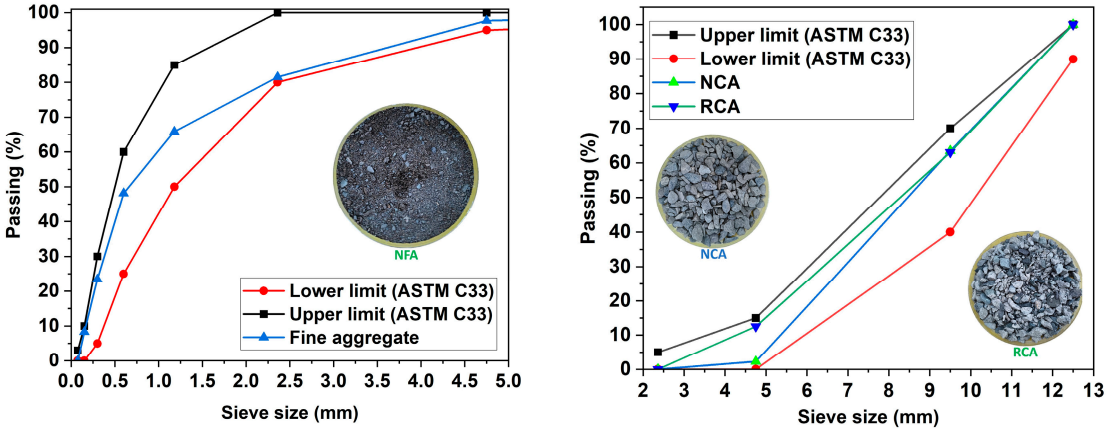

Figure 5. Percentage passing of NFA, NCA, and RCA.

Table 2. Physical and mechanical properties of NCA and RCA.

Characteristic	Standard	Aggregate	
		NCA	RCA
Density (kg/m^3)	ASTM C127 [50]	2620	2290
Water absorption (%)	ASTM C127 [50]	1.71	6.83
Nominal maximum size (mm)	ASTM C125 [51]	12.7	12.7
Abrasion resistance	ASTM C131 [52]	14.43	27.98

2.1. Concrete Mixture Designs

Five distinct concrete mixture designs were developed to investigate the effects of CS and RCA on the fresh and hardened properties of concrete. These mixtures incorporated varying levels of replacement for OPC with CS (0 and 15% by volume), and NCA with RCA (0, 20, 50, and 100% by volume). The 15% replacement level for OPC with CS was chosen based on prior research [3], which demonstrated that higher substitution rates resulted in significant compressive strength losses compared to a reference mixture containing 100% OPC. To ensure consistency in the mix design proportion, adjustments were made to the quantities of water and aggregates (natural and recycled), based on the actual moisture content of the aggregates. Table 3 presents the detailed proportions for each concrete mixture. It is important to note that the water content (196 kg/m^3), SP dosage (2.4 kg/m^3),

and NFA quantity (889.8 kg/m^3) were kept constant across all the mixtures. Additionally, corrections for aggregate (NFA, NCA, and RCA) moisture content were systematically performed.

Table 3. Mixture proportioning of concrete with CS and RCA, and identification code (ID).

Mixtures	MIX ID	Vol. Replacement Level (%) of NCA byRCA	OPC (kg/m^3)	SC (kg/m^3)	Water (kg/m^3)	NFA (kg/m^3)	NCA (kg/m^3)	RCA (kg/m^3)	SP (kg/m^3)
Reference	M1	0	400	0	196	889.8	830.9	0	2.4
15% CS	M2	0	340	71.4	196	889.8	830.9	0	2.4
15% CS–20% RCA	M3	20	340	71.4	196	889.8	664.7	145.2	2.4
15% CS–50% RCA	M4	50	340	71.4	196	889.8	415.4	363.1	2.4
15% CS–100% RCA	M5	100	340	71.4	196	889.8	0	726.2	2.4

The mixing process followed the following steps. (i) The NCA was pre-wetted by mixing it with water for 30 s, followed by a 300 s rest period to allow maximum water absorption by the NCA and/or RCA; (ii) sand was added and mixed for 60 s. (iii) The OPC was added and mixed for 120 s to homogenize all the particulate material. For the mixtures containing CS, OPC and CS were pre-mixed in a dry state before being introduced into the mixer. (iv) The water and the SP were added and mixed for 180 s (all the materials in the mix). (v) The mixer was stopped for two minutes, after which it was restarted for an additional 60 s. The homogenization of the mixture was checked at this stage.

For specimen preparation (cylindrical and prismatic specimens), molds were meticulously cleaned, and a release agent was applied a day prior to use. After filling the molds and compacting the mixtures, the specimens were leveled and left covered in the molds for 24 $\pm$ 2 h before demolding. Subsequently, they were submerged in lime-saturated water until the designated testing period.

2.2. Experimental Methods

A slump test of fresh mixture was performed in accordance with ASTM C 143 [53] to evaluate the influence of CS and RCA on the workability of the mixtures. In their hardened state, the compressive strength of the different mixtures was determined using cylindrical specimens (100 mm $\times$ 200 mm) tested with a universal testing machine, following the guidelines of ASTM C33 [54], at 7, 28, 120, and 180 days of curing. The splitting tensile strength of the concrete cylinders (100 mm $\times$ 200 mm) was assessed according to ASTM C496 specifications [55] at 28, 120, and 180 days of curing. The flexural strength of the different mixtures was evaluated using prismatic specimens (150 mm $\times$ 150 mm $\times$ 300 mm) in compliance with ASTM C293 [56] at 28 and 180 days of curing. Three concrete samples from each mixture and each curing age were used for the evaluation of each mechanical property.

In addition, the porosity and absorption, as well as the capillary suction, of the mixtures were evaluated based on ASTM C642 [57] and ASTM C1585 [58], respectively, for specimens cured for 28 and 180 days.

2.3. Carbon Footprint Analysis

Analysis of the carbon footprint of the designed concrete mixtures was performed by utilizing primary experimental data and secondary data extracted from the Inventory of Carbon and Energy (ICE) database [59]. The ICE provides a rigorous and dependable repository of data concerning embodied energy and carbon, offering extensive information on conventional construction materials within the cradle-to-gate boundary [60,61]. The analysis focused on estimating the emissions associated with the production of the raw

materials used in the concrete mixtures. Figure 6 illustrates the cradle-to-gate life cycle assessment (LCA) (modules A1–A3) for the concrete mixtures incorporating CS and RCA.

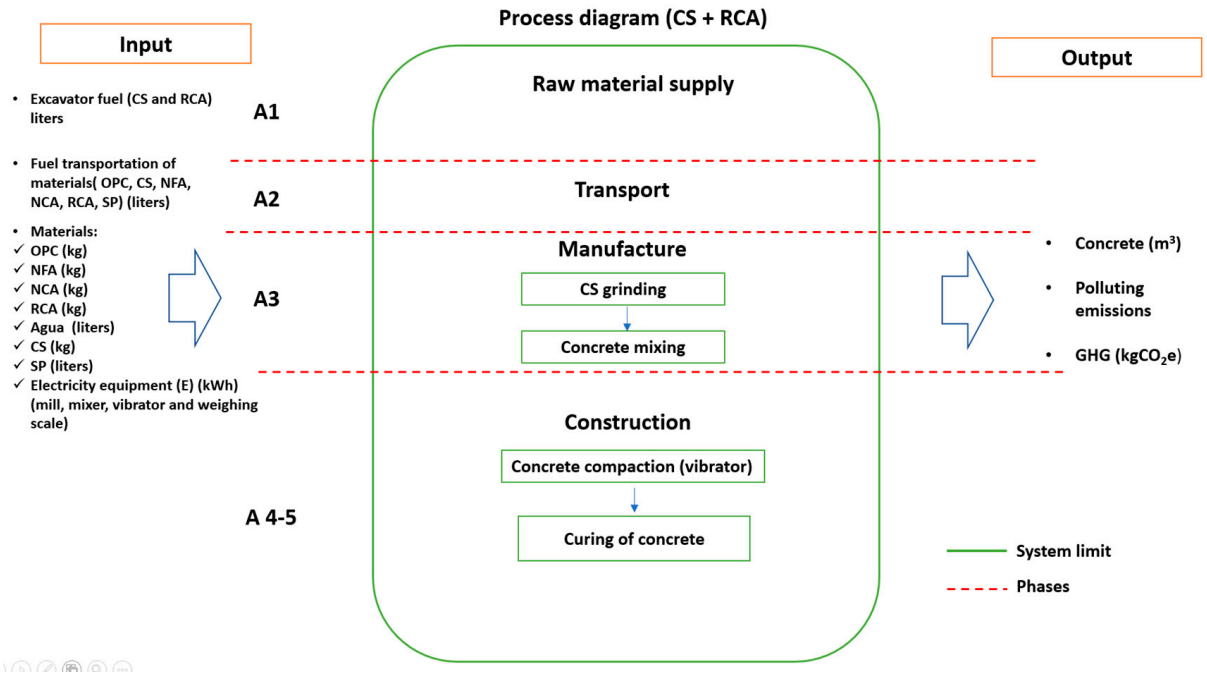

Figure 6. Processes included in this cradle-to-gate LCA study within the framework of the entire LCA of a construction project.

It is worth mentioning that the cradle-to-gate LCAs developed for each mixture did not account for the trade-off between the reduction in carbon footprint and loss in mechanical properties (expressed as kg·CO_2·eq and kg·CO_2·eq/MPa), including compressive strength, flexural strength, and indirect tensile strength. This trade-off analysis would require defining specific structural applications for the mixtures, which is beyond the scope of this study, and is recommended for future investigations.

3. Results

3.1. Slump Test

Figure 7 shows the effect on slump of CS and RCA in the mixtures (where the bars represent the average values, and the error bars indicate one standard deviation above and below the mean). The same representation is used in Figures 7–9, showing the results of the slump test performed on the different concrete mixtures. The substitution of OPC with CS (M2) resulted in an increase in slump when compared to the reference mixture with 100% OPC (M1). This behavior is attributed to the fact that CS exhibits poor water absorption due to its glassy texture. Additionally, the average particle size of CS (26.48 µm) was larger than that of OPC (17.37 µm), leading to the CS particles having a smaller specific surface area, and therefore requiring less water to wet their surface [62,63]. It is worth noting that further evaluations, such as particle packing density, could be conducted to assess the impact of CS reactivity and its contribution to the long-term strength of concrete. Such evaluations are recommended for future research.

On the other hand, for the concrete mixtures containing 50% and 100% RCA, there was a pronounced reduction in slump, indicating a loss in workability as the RCA content increased. The most significant reduction was observed in the mixture with 100% RCA (M5), with decreases of 17% and 24% compared to mixtures M1 and M2, respectively. The slump reduction observed in M4 and M5 is attributed to the angularity and surface roughness of the RCA, which are likely intensified by the crushing process [17,53].

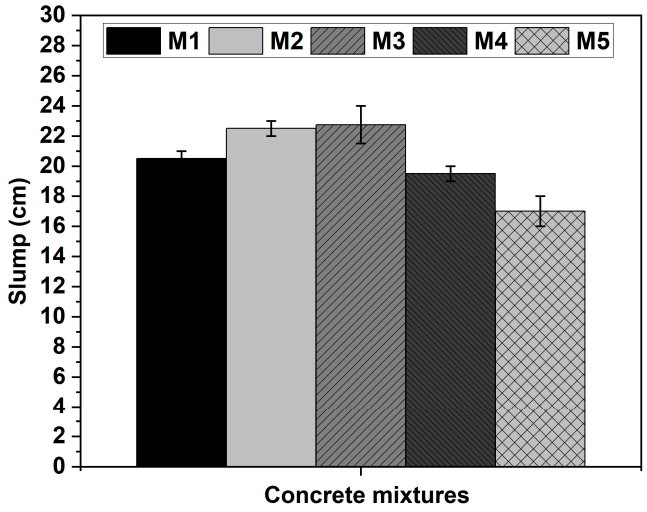

Figure 7. Effect on slump of the CS and RCA in concrete.

3.2. Compressive Strength

The influence of CS and RCA on the compressive strength of the different concrete mixtures is presented in Figure 8. It can be seen that the average strength of all the mixtures improved with prolonged curing, due to the increased degree of cement hydration and the contribution of CS as a cement substitute. These factors collectively generated a more compact microstructure [3,64]. Furthermore, as seen in Figure 8, when comparing the mixture with 100% OPC (M1) and the M2 mixture (in which only the OPC was replaced by 15% CS), a compressive strength reduction of 17.8%, 8.51%, and 1.93% was observed at 7, 28, and 120 days of curing, respectively. This early-age strength reduction can be attributed to the low pozzolanic reactivity of CS during early hydration, resulting in a dilution effect. The dilution effect of CS led to reduced C-S-H formation due to the lower alite and belite content of the mixture, as well as an increase in the effective water–cement ratio because CS has a lower water demand [49,65]. However, at a longer age (180 days of curing), the average compressive strength of M2 exhibited a 1.2% increase compared to M1.

On the other hand, the mixtures containing RCA (M3, M4, and M5), compared to the mixtures without RCA (M1 and M2), demonstrated a progressive strength decrease as the RCA content increased, at all the curing ages evaluated. At 28 days of curing, comparing mixtures M3, M4, and M5 with M2 revealed strength losses of 2.93%, 10.5%, and 15.4%, respectively. By 180 days of curing, this strength loss was more pronounced, ranging from 2.7% to 25%, when comparing the RCA mixtures with M2. This behavior is attributed to the influence of the old ITZ in RCA, which governs the concrete failure. The influence of the RCA became more pronounced as the strength of the new concrete mixtures exceeded the strength of the original concrete from which the RCA was derived.

In general, the strength reduction was caused by the adhered mortar in the RCA and the ITZ, which lowered the mechanical and physical quality of this type of aggregate. RCA typically has a lower density and Los Angeles abrasion resistance, as well as a higher absorption capacity and porosity [66]. Additionally, concrete mixtures with RCA exhibited two different ITZs: (i) between the natural aggregate and the old mortar; and (ii) between the RCA and the new cementitious matrix. These dual ITZs resulted in reduced strength, as the ITZ is considered the weakest region in concrete, and is where cracking typically initiates [67].

It is important to note that countries with developed construction standards have national guidelines or limits for maximum RCA content. For example, Australia, Brazil, and Germany limit the RCA content to 30%, 20%, and 25% or 35%, respectively, to balance mechanical performance and durability with the environmental benefits of reduced natural aggregate usage [68]. These recommended limits align with the performance observed in

mixture M3, the compressive strength of which remained largely unaffected by the use of 20% RCA.

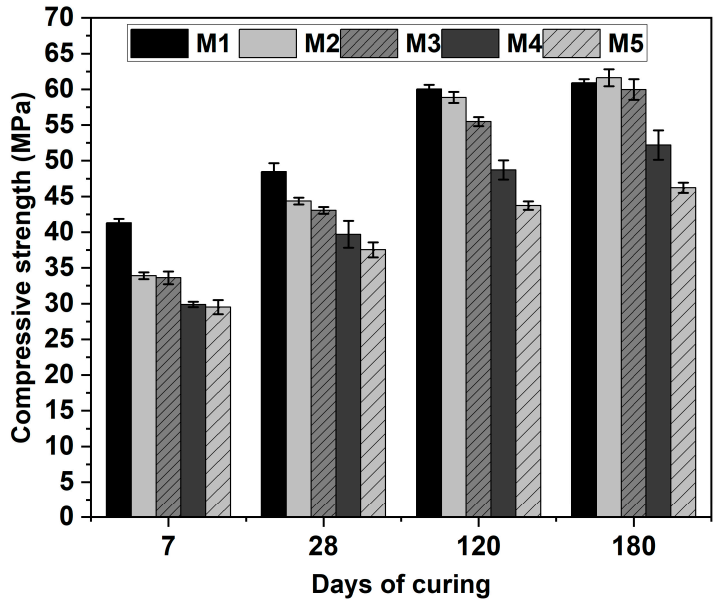

Figure 8. Compressive strength of concrete with CS and different proportions of RCA at different curing ages.

3.3. Splitting Tensile Strength

The evaluation of tensile strength helps to determine the stress level at which cracking leads to concrete failure [69,70]. Figure 9 presents the indirect tensile strength results for the different concrete mixtures. At 28 days of curing, the mixture with 15% CS (M2) showed a higher average strength compared to the reference mixture (M1), reaching 4.32 MPa (an increase of 4.1%). This behavior was maintained regardless of the curing time, despite the slow reaction rate of CS. This improvement is attributed to the sharp angular edges of CS particles, which enhances strength [3,31,71]. On the other hand, the concretes with RCA at 28 days of curing showed a progressive reduction in tensile strength as the RCA content increased. This behavior can be attributed to the weaker microstructure of RCA, caused by the adhered mortar on the original aggregate, in comparison with NCA [41]. Therefore, the volume of ITZ increased in the concrete mixtures as the RCA content increased, leading to a reduction in indirect tensile strength. At 28 and 180 days of curing, the concrete mixtures with 50% RCA (M4) and 100% RCA (M5) exhibited decreases of 9.5% and 14.8, and 5.25% and 11.98%, respectively, compared to the M2 mixture. In addition, it is important to note that mixture M3 exhibited the best tensile strength performance at prolonged curing ages (120 and 180 days). This behavior is attributed to the microstructural modifications in RCA pores [72,73], as well as the angularity and rougher surface of RCA, which generates a better mechanical interlocking between the cement paste and this type of aggregate, minimizing the negative effects of adhered mortar [74,75]. Furthermore, mixture M3 had a lower overall ITZ volume compared to M4 and M5. A similar behavior was observed by Megharani et al. [76], in whose study concrete mixtures containing 10–30% RCA demonstrated higher indirect tensile strengths than the reference mixture.

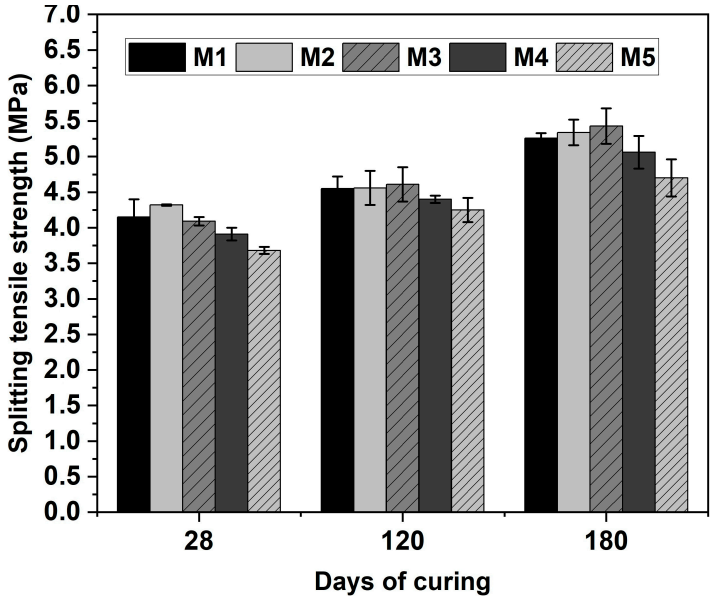

Figure 9. Splitting tensile strength of concrete with CS and different proportions of RCA at different curing ages.

3.4. Flexural Strength

The influence of CS and RCA on the flexural strength of the concrete mixtures at 28 and 180 days of curing is shown in Figure 10. At 28 days, a reduction in flexural strength was observed in the mixtures containing recycled materials (CS and RCA) compared to the reference mixture (M1). This reduction was more pronounced in the mixture with total replacement of NCA by RCA (M5), with a 15.2% decrease in flexural strength. However, this reduction in flexural strength was less severe than the compressive strength loss. This difference can be attributed to the greater angularity of the RCA, due to the adhered mortar, compared to the NCA. This angularity enhanced the bond between RCA and the new cementitious matrix, which is the primary factor affecting flexural strength [64,77].

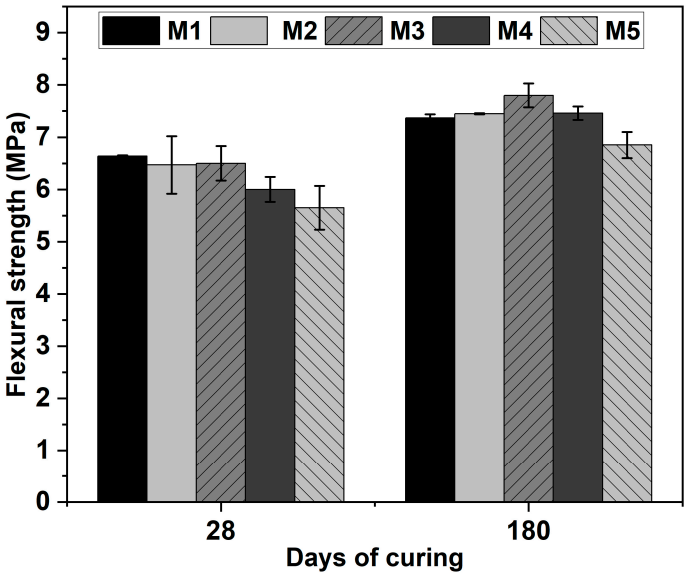

Figure 10. Flexural strength of concrete with CS and different proportions of RCA at different curing ages.

At 180 days of curing, the M3 mixture exhibited the best flexural performance among all mixtures, achieving a 5.8% higher strength than the reference mixture (M1). This improvement can be attributed to the continued development of flexural strength over time, which enhanced the adhesion between the new cementitious matrix and the RCA surface due to its higher roughness and the internal curing effect provided by RCA's higher water absorption capacity [78]. However, despite the improved performance of the new ITZ, when 100% RCA (M5) was used, the overall performance of the concrete mixture was largely governed by the quality of the RCA. This was due to the higher volume of interface in the mixture's composition. As a result, the RCA content in concrete designs requires special consideration.

3.5. Density, Absorption, and Voids

Table 4 presents the density, absorption, and voids test results of the different mixtures at 28 and 180 days of curing. At 28 days, it is evident that the use of CS resulted in an increase in density, attributed to the higher density of this material compared to OPC. A similar effect was observed with the use of RCA, which has lower density than NCA. The concrete mixtures exhibited progressively lower density values as the RCA content increased. This can be explained by the correlation between the macro porosity of the RCA [79] and the reduced density in the mixtures with this recycled material (RCA). Furthermore, this is also related to the greater water loss in mixtures with RCA due to their higher absorption capacity [80], which led to a higher average porosity ranging from 12.7% to 34.6%, and 10.47% to 31.9%, in comparison to M1 and M2 mixtures (concretes without RCA), respectively. A similar behavior was reported by Kapoor et al. [81], who observed greater water absorption in self-compacting concrete (SCC) containing 50% and 100% of RCA compared to SCC without RCA. At 180 days of curing, all the mixtures exhibited higher densities and reduced water absorption and voids adsorption compared to their 28 days counterparts. This improvement can be attributed to the increased degree of hydration in all the mixtures, that generated a higher formation of hydration products, such as C-S-H, which filled the pores, consequently decreasing water absorption and porosity [82].

Table 4. Water absorption, bulk density, and voids of concrete with CS and RCA.

Mixture (ID)	Water Absorption (%)		Bulk Density (kg/m^3)		Voids (%)	
	28	**180**	**28**	**180**	**28**	**180**
M1	7.77	5.22	2590	2616	17.05	11.28
M2	7.93	5.07	2610	2639	17.59	11.17
M3	8.76	5.16	2578	2619	18.65	11.43
M4	9.63	6.82	2510	2543	19.34	14.16
M5	10.46	7.59	2463	2480	19.66	15.46

3.6. Capillary Water Absorption (Sorptivity)

Figure 11 presents the initial and secondary absorption rates of the different concrete mixtures at 28 and 180 days of curing. These rates are essential coefficients for estimating the service life of concrete, with a lower sorptivity value indicating an increase in service life [83]. In Figure 11a, it can be observed that the use of CS and RCA in the design of the concrete mixtures led to an increase in the rate of capillary water absorption at 28 days. When comparing mixture M1 to the other concrete mixtures, the initial water absorption rate increased from 1.8% to 52.6% with the use of CS and the total replacement of NCA by RCA, with the lowest rate being 0.0116 mm/s$^{1/2}$ and the highest rate being 0.0177 mm/s$^{1/2}$ for M1 and M5, respectively. The presence of high amounts of RCA significantly influenced the increase in the amount of water absorbed. The increased sorptivity in mixtures containing recycled materials can be attributed to their pore structure, higher

effective porosity [71], and the dilution effect [84] caused at 28 days of curing by the partial replacement of OPC with CS.

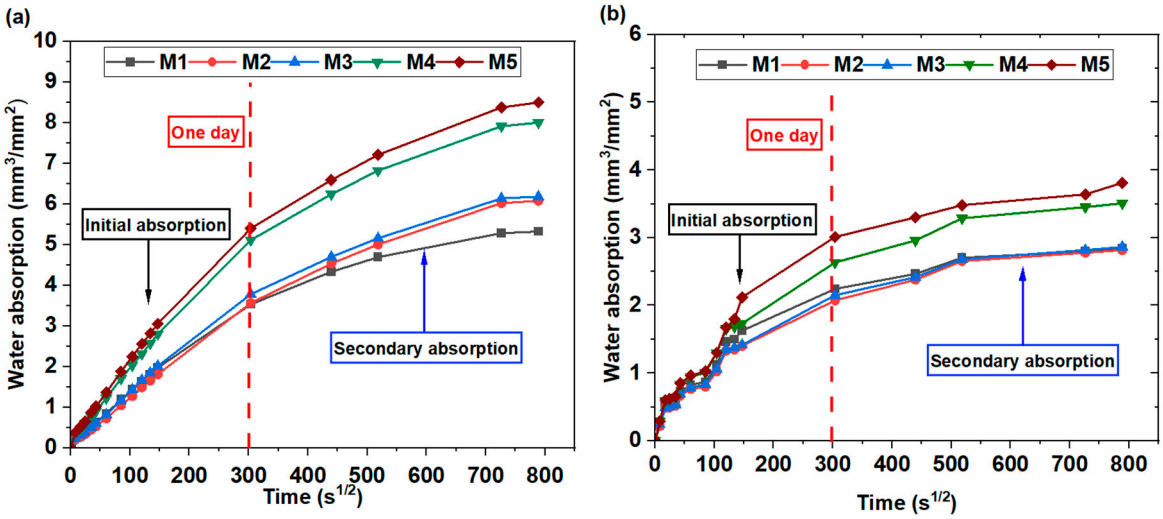

Figure 11. Water absorption of different concrete mixtures, (**a**) 28 days and (**b**) 180 days of curing.

At 180 days of curing (Figure 11b), a reduction in capillary water absorption was observed in all the mixtures. In detail, the capillary water absorption values at 180 days for M1 to M5 were 39.8%, 43.4%, 45.4%, 50.2%, and 45.4%, when compared to their counterparts cured for 28 days, respectively. These reductions were due to adequate curing, which promoted a higher degree of hydration of the OPC, resulting in greater formation of C-S-H gels, which reduced the capillary pores and improved the resistance to water access [85]. In addition, at 180 days of curing, the beneficial effect of CS as an SCM was seen, as it contributed to a more refined capillary pore structure, leading to reduced water absorption [3].

3.7. Carbon Footprint Results of the Concrete Mixtures

As outlined in the methodology in Section 2.3, the embodied carbon (EC) of each concrete mixture was estimated using a cradle-to-gate LCA approach encompassing modules A1 to A3, as illustrated in Figure 6. As previously mentioned, these mixtures incorporate 15% recycled CS as a replacement for OPC, and varying proportions of crushed recycled concrete as aggregate at 0%, 20%, 50%, and 100% substitution levels. Recognizing that transportation distances significantly contribute to environmental impacts [86], two production scenarios were analyzed. The first scenario assumed concrete production in Santiago (Chile), which had specific distances from the cement plant and the CS supplier. The second scenario considered concrete production in Viña del Mar (Chile), reflecting different transportation distances. These scenarios were chosen to represent the current locations of material suppliers and to assess how transportation distances affect overall environmental impacts. For RCA, a maximum acquisition radius of 5 km within each city was assumed. The locations analyzed are depicted in Figure 12, in which the CS supplier is marked with a red icon, the nearby cement plants are marked with yellow icons, and the cities are marked with blue icons.

Considering these two scenarios, Figure 13 illustrates the corresponding results for the EC assessment. The data show that producing concrete with recycled components in Santiago does not result in significant environmental benefits compared to production in Viña del Mar, which is located closer to material suppliers. In the optimal case for the Viña del Mar location, a reduction of approximately 6% in EC was observed when CS was added to the mixture and no natural aggregate was used. This highlights the significant impact of transport distances on the EC of construction materials. Furthermore, the analysis of RCA substitution for Viña del Mar revealed that substituting NCA with RCA did not

significantly reduce the carbon footprint. Notably, as the substitution rate increased from 0% to 100%, emissions slightly increased. This finding aligns with previous research, which found that replacing NCA with RCA at proportions of 50% and 100% leads to higher carbon emissions [87]. However, some studies report contradictory results, showing that CO_2 generation per m^3 of concrete can decrease with the use of RCA [8,88].



Figure 12. Locations of the CS supplier (red mark) and cement plant (yellow mark), and the cities in which concrete mixtures are assumed to be produced (blue mark). Obtained from Google Maps.

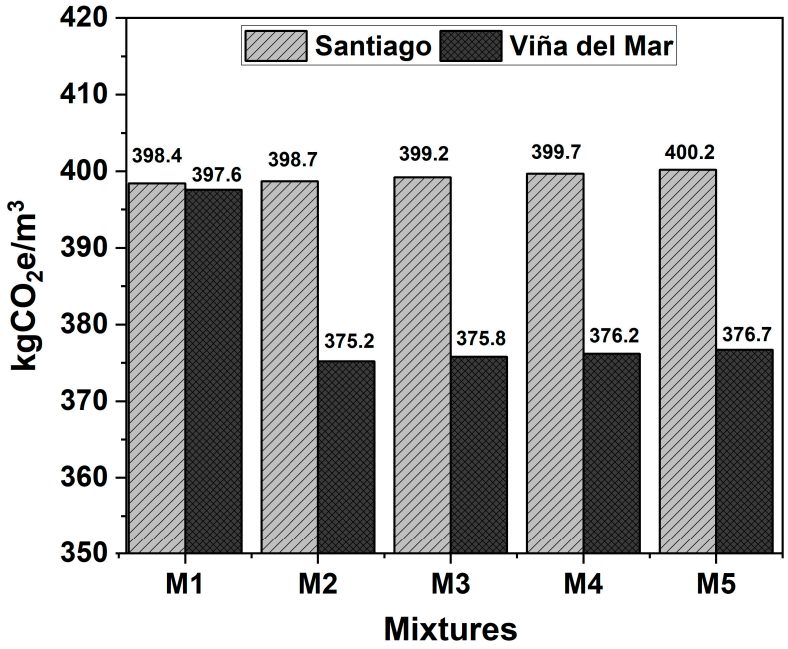

Figure 13. Comparison of the embodied carbon in the mixtures with CA–RCA and the reference mixture.

Therefore, depending on transport distances, the most significant reductions in EC were achieved by substituting only the cement constituent, which accounts for nearly 95% of the carbon burden in concrete [89], with CS. The impact of the amount of OPC

has been widely recognized in several studies [90,91], indicating that the EC is mainly influenced by the binder phase. Consequently, greater reductions in EC could be achieved with higher levels of OPC substitution. This highlights the advantages of using locally sourced by-products or waste materials with pozzolanic activity as partial cement substitutes, which offers both environmental and economic benefits [92]. On the other hand, the results indicate that incorporating RCA materials into concrete does not always yield environmental benefits. To achieve substantial reductions in concrete-related emissions, focus should be placed on replacing cement, minimizing transport distances, and reducing the carbon emission factors associated with energy use, both in transportation and manufacturing processes. For instance, utilizing clean energy in the crushing of recycled aggregate and the grinding of CS will result in lower associated carbon emissions. This is particularly important because the emissions associated with the grinding process in the study accounted for 6.7% to 7.3% of the total carbon emissions across the analyzed mixtures. These considerations should guide decision-making regarding the selection of raw materials and energy sources for construction products.

It is crucial to highlight that carbon emissions are strongly influenced by the manufacturing process and the type of energy used (e.g., transportation by truck and operational activities), leading to significant variations in carbon emissions related to materials [91], and recycling constituents for concrete production is not an exception to this. As shown in Figure 13, the resulting emission rates ranged from a minimum of 375.2 $kgCO_2e/m^3$ to a maximum of 400.2 $kgCO_2e/m^3$. According to previous research, these values fall within the expected range for concrete that incorporates recycled constituents [92].

In addition to the calculation of $kgCO_2{\cdot}eq$, the ratio of $kg{\cdot}CO_2{\cdot}eq/MPa$ was determined, considering the compressive strength at 28 and 180 days of curing, as illustrated in Figure 14. This behavior was evaluated in three concrete mixtures (M1, M2, and M5), which showed lower values of $kgCO_2{\cdot}eq/MPa$ at 180 days due to the development of hydration products and pozzolanic reactions evident at longer curing ages. At 28 days of curing, the lowest $kg{\cdot}CO_2{\cdot}eq/MPa$ values were presented by mixture M1, since it had the highest compressive strength. However, after 180 days of curing, mixture M2 exhibited the lowest value, as it had the highest compressive strength at this age, while also generating the least $kg{\cdot}CO_2{\cdot}eq$ in Viña del Mar, with its application close to the CS source. In contrast, the M5 mixture (with CS and 100% RCA), at both curing ages, showed the highest $kgCO_2{\cdot}eq/MPa$ ratio. This is because the use of RCA as a total replacement for NCA leads to a loss of compressive strength.

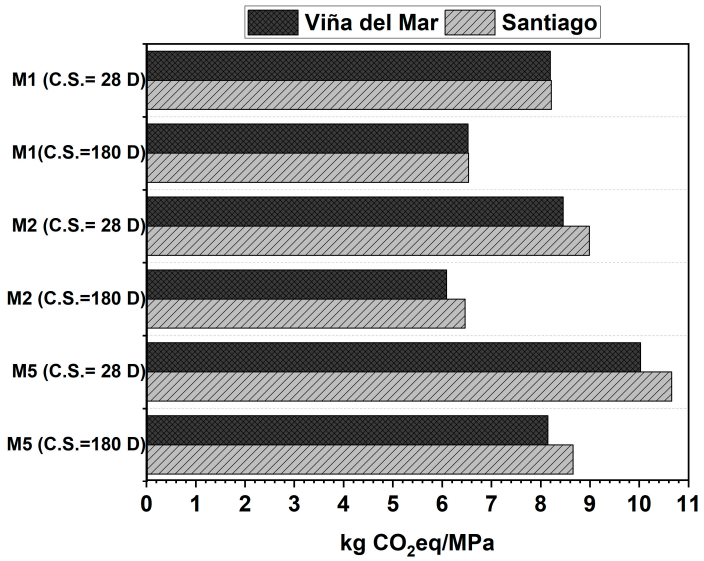

Figure 14. $kg{\cdot}CO_2{\cdot}eq/MPa$ ratio calculated for concretes M1, M2, and M5.

4. Conclusions

This study investigated the fresh and hardened performance (both short- and long-term) of concrete mixtures with the combined partial replacement of ordinary Portland cement (OPC) with copper slag (CS), and of natural coarse aggregate (NCA) with recycled coarse aggregate (RCA) from concrete construction and demolition waste (CDW), and analyzed the embodied carbon (EC) of each mixture. This research confirms that it is feasible to use CS as a supplementary cementitious material (SCM) partially replacing OPC, and to use RCA as replacement for NCA, in the same concrete mixture. Based on the experimental results and analysis of this research, the following conclusions can be made:

- The replacement of 15% by vol. of OPC with CS is viable, despite the dilution effect that results in a loss of compressive strength at early ages (7 and 28 days of curing). However, at longer curing periods (120 and 180 days), the difference in compressive strength between the 100% OPC mixture (M1) and the 15% CS mixture (M2) became insignificant. Notably, at 180 days, mixture M2 achieved an average compressive strength that was slightly higher (1.2%) compared to M1.
- The favorable performances of the M2 and M3 (15% CS and 20% RCA) mixtures in terms of indirect tensile strength and flexural strength suggest potential applications in engineering contexts, such as pavements, for which concrete flexural strength performance is critical. This improvement can be explained by the increased angularity and roughness of CS and RCA, compared to OPC and NCA, respectively.
- The negative effect of RCA on the mechanical properties of concrete was most significant in terms of compressive strength performance, compared to indirect tensile and flexural strength performance. For example, after 180 days of curing, when comparing mixture M2 (15% CS and 0% RCA) with M5 (15% CS and 100% RCA), the compressive, indirect tensile, and flexural strengths decreased by 24.1%, 11.98%, and 8.05%, respectively.
- Porosity, absorption, and sorptivity were negatively affected by high RCA contents (50% and 100%) in the concrete mixtures at both the evaluated ages (28 and 180 days of curing). However, mixture M2 (15% CS and 0% RCA) exhibited 2.87% less porosity at 180 days of curing compared to the reference mixture (M1), which can be attributed to the slow pozzolanic effect of CS.
- From the EC analyses, major environmental benefits were obtained through partially replacing OPC with CS, while the substitution of NCA with RCA had a minor impact.
- The development of more sustainable concrete mixtures can be achieved with higher substitution rates of OPC with CS. However, it is essential to address the low reactivity of CS. Striking a balance between CO_2 emission reduction and potential impacts on mechanical performance and durability is crucial. Additionally, future research should focus on methods to enhance the reactivity of CS in cementitious matrices, optimizing its performance as an SCM.

Author Contributions: Conceptualization, P.W.C.A., Y.F.S., G.A.-L. and H.H.; methodology, P.W.C.A., Y.F.S. and G.A.-L.; Software, Y.F.S.; validation, P.W.C.A., Y.F.S., G.A.-L. and H.H.; formal analysis, P.W.C.A., Y.F.S., G.A.-L. and H.H.; investigation, P.W.C.A., Y.F.S., G.A.-L.; resources, Y.F.S.; data curation, P.W.C.A., Y.F.S. and G.A.-L.; writing—original draft preparation, P.W.C.A., Y.F.S., G.A.-L. and H.H.; writing—review and editing, Y.F.S. and G.A.-L. visualization, Y.F.S. and G.A.-L.; supervision, Y.F.S. and G.A.-L.; project administration, Y.F.S.; funding acquisition, Y.F.S. All authors have read and agreed to the published version of the manuscript.

Funding: This research was funded by Fondecyt de Iniciación N°11221114 and The APC was funded by Fondecyt de Iniciación.

Institutional Review Board Statement: Not applicable.

Informed Consent Statement: Not applicable.

Data Availability Statement: The data presented in this research are available on request from the corresponding author.

Acknowledgments: The authors would like to acknowledge the support of the Agencia Nacional de Investigación y Desarrollo (ANID) through grant FONDECYT iniciacion' #11221114, the Academic Insertion Program of the Pontificia Universidad Católica de Chile (PIA UC), the Concrete Innovation Hub UC (CIHUC), Codelco, and Sika.

Conflicts of Interest: The authors declare no conflict of interest.

Nomenclature

Al_2O_3	Alumina
CaO	Limestone
CDW	Construction and demolition waste
CO_2	Carbon dioxide
CS	Copper slag
EC	Embodied carbon
FA	Fly ash
Fe_2O_3	Iron oxide
GGBFS	Granulated blast-furnace slag
ICE	Inventory of Carbon and Energy
ID	Identification code of concrete mixtures
NCA	Natural coarse aggregate
NFA	Natural fine aggregate
M1	Concrete mixture with 100% OPC
M2	Concrete mixture with 15% CS
M3	Concrete mixture with 15% CS and 20% RCA
M4	Concrete mixture with 15% CS and 50% RCA
M5	Concrete mixture with 15% CS and 100% RCA
MgO	Magnesium oxide
ITZ	Interfacial transition zone
LOI	Loss on ignition
LCA	Life cycle assessment
OPC	Ordinary Portland cement
SCM	Supplementary cementitious material
SiO_2	Silica
RCA	Recycled coarse aggregate
SP	Super plasticizer
XRF	X-ray fluorescence

References

1. Raghuvanshi, H.; Singh, N. Fresh and Mechanical Properties of Ground Granulated Blast Furnace Slag-Based Concrete: A Review. *Mater. Today Proc.* **2024**, *193*. [CrossRef]
2. Li, L.; Joseph, P.; Zhang, X.; Zhang, L. A Study of Some Relevant Properties of Concrete Incorporating Waste Ceramic Powder as a Cement Replacement Agent. *J. Build. Eng.* **2024**, *87*, 109106. [CrossRef]
3. Silva, Y.F.; Burbano-Garcia, C.; Araya-Letelier, G.; González, M. Short- and Long-Term Experimental Performance of Concrete with Copper Slag: Mechanical and Physical Properties Assessment. *Case Stud. Constr. Mater.* **2024**, *20*, e03302. [CrossRef]
4. Chen, X.; Zhang, D.; Cheng, S.; Xu, X.; Zhao, C.; Wang, X.; Wu, Q.; Bai, X. Sustainable Reuse of Ceramic Waste Powder as a Supplementary Cementitious Material in Recycled Aggregate Concrete: Mechanical Properties, Durability and Microstructure Assessment. *J. Build. Eng.* **2022**, *52*, 104418. [CrossRef]
5. Vintimilla, C.; Etxeberria, M.; Li, Z. Durable Structural Concrete Produced with Coarse and Fine Recycled Aggregates Using Different Cement Types. *Sustainability* **2023**, *15*, 14272. [CrossRef]
6. Abellan-Garcia, J.; Fernández-Gómez, J.; Iqbal Khan, M.; Abbas, Y.M.; Pacheco-Bustos, C. ANN Approach to Evaluate the Effects of Supplementary Cementitious Materials on the Compressive Strength of Recycled Aggregate Concrete. *Constr. Build. Mater.* **2023**, *402*, 132992. [CrossRef]
7. Zhu, P.; Wang, H.; Yan, X.; Yang, L.; Zhu, L.; Liu, H. Recycled Coarse Aggregate from Parent Concrete with Supplementary Cementitious Materials under Freeze-Thaw Environment: Recyclability, Environment and Economic Evaluation. *J. Build. Eng.* **2024**, *84*, 108699. [CrossRef]
8. Xing, W.; Tam, V.W.; Le, K.N.; Hao, J.L.; Wang, J. Life Cycle Assessment of Sustainable Concrete with Recycled Aggregate and Supplementary Cementitious Materials. *Resour. Conserv. Recycl.* **2023**, *193*, 106947. [CrossRef]

9. Rodriguez-Morales, J.; Burciaga-Diaz, O.; Gomez-Zamorano, L.Y.; Escalante-Garcia, J.I. Transforming Construction and Demolition Waste Concrete as a Precursor in Sustainable Cementitious Materials: An Innovative Recycling Approach. *Resour. Conserv. Recycl.* **2024**, *204*, 107474. [CrossRef]
10. Li, J.; Wang, T.; Du, C.; Wang, C.; Cao, F.; Su, T. Multi-Faceted Assessment of Microbial-Reinforced Recycled Brick Aggregate Concrete. *Chem. Eng. J.* **2024**, *497*, 154481. [CrossRef]
11. Kalinowska-Wichrowska, K.; Kosior-Kazberuk, M.; Pawluczuk, E. The Properties of Composites with Recycled Cement Mortar Used as a Supplementary Cementitious Material. *Materials* **2020**, *13*, 64. [CrossRef] [PubMed]
12. Golafshani, E.M.; Behnood, A.; Kim, T.; Ngo, T.; Kashani, A. A Framework for Low-Carbon Mix Design of Recycled Aggregate Concrete with Supplementary Cementitious Materials Using Machine Learning and Optimization Algorithms. *Structures* **2024**, *61*, 106143. [CrossRef]
13. Degefa, A.B.; Park, S.; Yang, B.; Park, S. Predicting the Degree of Reaction of Supplementary Cementitious Materials in Hydrated Portland Cement. *Sustainability* **2023**, *15*, 15471. [CrossRef]
14. Bouzar, B.; Mamindy-Pajany, Y. Immobilization Study of As, Cr, Mo, Pb, Sb, Se and Zn in Geopolymer Matrix: Application to Shooting Range Soil and Biomass Fly Ash. *Int. J. Environ. Sci. Technol.* **2023**, *20*, 11891–11912. [CrossRef]
15. Silva, Y.F.; Delvasto, S.; Izquierdo, S.; Araya-Letelier, G. Short and Long-Term Physical and Mechanical Characterization of Self-Compacting Concrete Made with Masonry and Concrete Residue. *Constr. Build. Mater.* **2021**, *312*, 125382. [CrossRef]
16. Hasheminezhad, A.; King, D.; Ceylan, H.; Kim, S. Comparative Life Cycle Assessment of Natural and Recycled Aggregate Concrete: A Review. *Sci. Total Environ.* **2024**, *950*, 175310. [CrossRef]
17. Bheel, N.; Chohan, I.M.; Ghoto, A.A.; Abbasi, S.A.; Tag-eldin, E.M.; Almujibah, H.R.; Ahmad, M.; Benjeddou, O.; Gonzalez-Lezcano, R.A. Synergistic Effect of Recycling Waste Coconut Shell Ash, Metakaolin, and Calcined Clay as Supplementary Cementitious Material on Hardened Properties and Embodied Carbon of High Strength Concrete. *Case Stud. Constr. Mater.* **2024**, *20*, e02980. [CrossRef]
18. Silva, Y.F.; Lange, D.A.; Delvasto, S. Effect of Incorporation of Masonry Residue on the Properties of Self-Compacting Concretes. *Constr. Build. Mater.* **2019**, *196*, 277–283. [CrossRef]
19. Silva, Y.F.; Villaquirán-Caicedo, M.; Izquierdo, S. Exploring the Potential of Alternative Materials in Concrete Mixtures: Effect of Copper Slag on Mechanical Properties and Carbonation Resistance. *Materials* **2023**, *16*, 6677. [CrossRef]
20. Perera, M.A.G.P.; Ranjith, P.G. Eco-Friendly Cementitious Composites for Enhanced Strength: Emerging Trends and Innovations. *J. Clean. Prod.* **2024**, *468*, 142962. [CrossRef]
21. Silva, Y.F.; Ph, D.; Delvasto, S.; Ph, D.; Valencia, W.; Ph, D.; Araya-letelier, G. Performance of Self-Compacting Concrete with Residue of Masonry and Recycled Aggregate under Sulfate Attack. *J. Mater. Civ. Eng.* **2024**, *36*, 1–12. [CrossRef]
22. Görhan, G.; Bozkurt, A.M. Investigation of Properties of Mortar Containing Pyrogenic Silica-Added Supplementary Cementitious Materials. *Rev. Constr.* **2022**, *2*, 118–134. [CrossRef]
23. Bouzar, B.; Mamindy-Pajany, Y. Manufacture and Characterization of Carbonated Lightweight Aggregates from Waste Paper Fly Ash. *Powder Technol.* **2022**, *406*, 117583. [CrossRef]
24. Ash, F.; Pv, S.; Poyyamozhi, M.; Murugesan, B.; Narayanamoorthi, R. Sustainable Concrete Roof Tiles: Integrating Aluminium Foil. *Sustainability* **2024**, *16*, 8257. [CrossRef]
25. Venkitasamy, V.; Santhanam, M.; Rao, B.P.C.; Balakrishnan, S.; Kumar, A. Mechanical and Durability Properties of Structural Grade Heavy Weight Concrete with Fly Ash and Slag. *Cem. Concr. Compos.* **2024**, *145*, 105362. [CrossRef]
26. Narendra Kumar, B.; Rushikesh, M.; Akhil Kumar, A. An Experimental Study on High Strength Self-Compacting Concrete Inclusion of Zeolite and Silica Fume as a Potential Alternative Sustainable Cementitious Materials. *Mater. Today Proc.* **2024**. [CrossRef]
27. Chandra Sekhar, M.; Kumar, M.H.; Lova Raju, S.; Saikrishnamacharyulu, I. Influence of Metakaolin and Glass Powder on Mechanical Behaviour of Concrete. *Mater. Today Proc.* **2023**. [CrossRef]
28. Rosado, S.; Gullón, L.; Martínez, L.F.M.; Llamas Borrajo, J.F. Potential Uses of Copper Wastes in the Building Sector: Inertization and Added Value Solutions. *Mater. Proc.* **2021**, *5*, 5025. [CrossRef]
29. Edwin, R.S.; Gruyaert, E.; De Belie, N. Valorization of Secondary Copper Slag as Aggregate and Cement Replacement in Ultra-High Performance Concrete. *J. Build. Eng.* **2022**, *54*, 104567. [CrossRef]
30. Mousavi, S.R.; Bahrpeyma, A.; Afshoon, I.; Chakkoshi, M. Protecting the Environment and Natural Resources Using Green Roller Compacted Concrete (RCC) Containing Fine and Coarse Recycled Copper Slag Aggregates. *Process Saf. Environ. Prot.* **2024**, *186*, 664–678. [CrossRef]
31. Sahu, A.; Kumar, S.; Srivastava, A.K.L.; Pratap, B. Performance of Recycled Aggregate Concrete Using Copper Slag as Fine Aggregate. *J. Build. Eng.* **2024**, *82*, 108364. [CrossRef]
32. Velumani, M.; Gowtham, S.; Dhananjayan, M.P.; Eniyan, G.T. Strength Assessment of Concrete with Copper Slag as Fine Aggregates. *Mater. Today Proc.* **2023**. [CrossRef]
33. Arunchaitanya, S.; Dey, S. Sorptivity and Rapid Chloride Ion Penetration of Self-Compacting Concrete Using Fly Ash and Copper Slag. *AI Civ. Eng.* **2023**, *2*, 4. [CrossRef]
34. Li, J.; Liao, Y.; Ma, H.; Liu, Q.; Wu, Y. Review on Comprehensive Recovery Valuable Metals and Utilization of Copper Slag. *J. Sustain. Metall.* **2023**, *9*, 439–458. [CrossRef]

35. He, R.; Zhang, S.; Zhang, X.; Zhang, Z.; Zhao, Y.; Ding, H. Copper Slag: The Leaching Behavior of Heavy Metals and Its Applicability as a Supplementary Cementitious Material. *J. Environ. Chem. Eng.* **2021**, *9*, 105132. [CrossRef]
36. Gopalakrishnan, R.; Nithiyanantham, S. Microstructural, Mechanical, and Electrical Properties of Copper Slag Admixtured Cement Mortar. *J. Build. Eng.* **2020**, *31*, 101375. [CrossRef]
37. Mirhosseini, S.R.; Fadaee, M.; Tabatabaei, R.; Fadaee, M.J. Mechanical Properties of Concrete with Sarcheshmeh Mineral Complex Copper Slag as a Part of Cementitious Materials. *Constr. Build. Mater.* **2017**, *134*, 44–49. [CrossRef]
38. Moghaddas, S.A.; Nekoei, M.; Mohammadi Golafshani, E.; Nehdi, M.; Arashpour, M. Modeling Carbonation Depth of Recycled Aggregate Concrete Using Novel Automatic Regression Technique. *J. Clean. Prod.* **2022**, *371*, 133522. [CrossRef]
39. Ren, X.; Yang, J.; Chen, W.; Huang, Y.; Wang, G.; Niu, J. Effect of Recycled Concrete Powder-Cement Composite Coating Modification on the Properties of Recycled Concrete Aggregate and Its Concrete. *Constr. Build. Mater.* **2024**, *444*, 137860. [CrossRef]
40. Haq, M.A.U.; Xia, P.; Khan, S.; Hassam, M.; Sohaib, M.; Gong, F.; Zhao, Y. Optimal Utilization of Low-Quality Construction Waste and Industrial Byproducts in Sustainable Recycled Concrete. *Constr. Build. Mater.* **2024**, *428*, 136362. [CrossRef]
41. Wang, J.; Che, Z.; Zhang, K.; Fan, Y.; Niu, D.; Guan, X. Performance of Recycled Aggregate Concrete with Supplementary Cementitious Materials (Fly Ash, GBFS, Silica Fume, and Metakaolin): Mechanical Properties, Pore Structure, and Water Absorption. *Constr. Build. Mater.* **2023**, *368*, 130455. [CrossRef]
42. Wang, J.; Fan, Y.; Che, Z.; Zhang, K.; Niu, D. Study on the Durability of Eco-Friendly Recycled Aggregate Concrete with Supplementary Cementitious Materials: The Combined Action of Compound Salt Solution of MgSO4, Na2SO4, and NaCl and Dry-Wet Cycles. *Constr. Build. Mater.* **2023**, *377*, 131149. [CrossRef]
43. Xia, G.; Zhao, Y. Interface Parameters of Recycled Aggregate Concrete Considering the Distribution of Old Mortar Content. *Case Stud. Constr. Mater.* **2024**, *20*, e03262. [CrossRef]
44. *ASTM C150*; Standard Specification for Portland Cement. ASTM International: West Conshohocken, PA, USA, 2022; pp. 1–9.
45. Barros, K.S.; Vielmo, V.S.; Moreno, B.G.; Riveros, G.; Cifuentes, G.; Bernardes, A.M. Chemical Composition Data of the Main Stages of Copper Production from Sulfide Minerals in Chile: A Review to Assist Circular Economy Studies. *Minerals* **2022**, *12*, 250. [CrossRef]
46. Payá, J.; Monzó, J.; Borrachero, M.V.; Velázquez, S.; Bonilla, M. Evaluation of the Pozzolanic Activity of Fluid Catalytic Cracking Catalyst Residue (FC3R). Thermogravimetric Analysis Studies on FC3R-Portland Cement Pastes. *Cem. Concr. Res.* **2003**, *33*, 603–609. [CrossRef]
47. Silva, Y.F.; Izquierdo, S.R.; Delvasto, S. Effect of Masonry Residue on the Hydration of Portland Cement Paste. *DYNA* **2019**, *86*, 367–377. [CrossRef]
48. *ASTM C127*; Standard Test Method for Relative Density (Specific Gravity) and Absorption of Coarse Aggregate. ASTM International: West Conshohocken, PA, USA, 2024; pp. 1–6.
49. *ASTM C125*; Standard Terminology Relating to Concrete and Concrete Aggregates. ASTM International: West Conshohocken, PA, USA, 2021; pp. 1–9.
50. *ASTM C131-20*; Standard Test Method for Resistance to Degradation of Small-Size Coarse Aggregate by Abrasion and Impact in the Los Angeles Machine. ASTM International: West Conshohocken, PA, USA, 2020.
51. *ASTM C143/C143M-20*; Standard Test Method for Slump of Hydraulic-Cement Concrete. ASTM International: West Conshohocken, PA, USA, 2020; Voulume 4, pp. 1–10.
52. *ASTM C39/C39M-18*; Standard Test Method for Compressive Strength of Cylindrical Concrete Specimens. ASTM International: West Conshohocken, PA, USA, 2018.
53. *ASTM C496/C496M−17*; Standard Test Method for Splitting Tensile Strength of Cylindrical Concrete Specimens. ASTM International: West Conshohocken, PA, USA, 2017; pp. 1–5.
54. *ASTM C293*; Standard Test Method for Flexural Strength of Concrete (Using Simple Beam with Third-Point Loading). ASTM International: West Conshohocken, PA, USA, 2016; pp. 1–4.
55. *ASTM C642-21*; Standard Test Method for Density, Absorption, and Voids in Hardened Concrete. ASTM International: West Conshohocken, PA, USA, 2021.
56. *ASTM C1585-20*; Standard Test Method for Measurement of Rate of Absorption of Water by Hydraulic Cement Concretes. ASTM International: West Conshohocken, PA, USA, 2020; pp. 1–6.
57. Hammond, G.; Jones, C. *Embodied Carbon, The Inventory of Carbon and Energy (Ice)*; University of Bath with BSRIA, ICAT: Elkridge, MD, USA, 2011.
58. Luciano, A.; Altamura, P.; Baiani, S.; Cutaia, L. The Building Stock as an Urban Mine: The Case of the Circular Regeneration of Disused Buildings. *Sustain. Chem. Pharm.* **2023**, *33*, 101104. [CrossRef]
59. Hernández, H.; Ossio, F.; Silva, M. Assessment of Sustainability and Efficiency Metrics in Modern Methods of Construction: A Case Study Using a Life Cycle Assessment Approach. *Sustainability* **2023**, *15*, 6267. [CrossRef]
60. Edwin, R.S.; Gruyaert, E.; De Belie, N. Influence of Intensive Vacuum Mixing and Heat Treatment on Compressive Strength and Microstructure of Reactive Powder Concrete Incorporating Secondary Copper Slag as Supplementary Cementitious Material. *Constr. Build. Mater.* **2017**, *155*, 400–412. [CrossRef]
61. Devi, S.C.; Khan, R.A. Effect of Graphene Oxide on Mechanical and Durability Performance of Concrete. *J. Build. Eng.* **2020**, *27*, 101007. [CrossRef]

62. Belabbas, O.; Bouziadi, F.; Boulekbache, B.; Hamrat, M.; Haddi, A.; Amziane, S. Mechanical Properties of Multi-Recycled Coarse Aggregate Concrete, with Particular Emphasis on Experimental and Numerical Assessment of Shrinkage at Different Curing Temperatures. *J. Build. Eng.* **2024**, *89*, 109333. [CrossRef]
63. Araos, P.; Aponte, D.; Barra, M. Ladle Furnace Slag as a New Source of Supplementary Cementitious Material: Evaluating Long-Term Performance and Environmental Impact in Portland Cement Systems. *J. Build. Eng.* **2024**, *95*, 109995. [CrossRef]
64. Reddy, V.S.; Shrihari, S.; Uma, P.; Kalyan, J.P. Treated Recycled Coarse Aggregate Concrete: A New Mixture Proportioning Method Based on Packing Densities. *Mater. Today Proc.* **2023**, 1–9. [CrossRef]
65. Trento, D.; Faleschini, F.; Revilla-Cuesta, V.; Ortega-López, V. Improving the Early-Age Behavior of Concrete Containing Coarse Recycled Aggregate with Raw-Crushed Wind-Turbine Blade. *J. Build. Eng.* **2024**, *92*, 109815. [CrossRef]
66. Lu, L. Optimal Replacement Ratio of Recycled Concrete Aggregate Balancing Mechanical Performance with Sustainability: A Review. *Buildings* **2024**, *14*, 2204. [CrossRef]
67. Neville, A. Properties of Concrete. PEARSON: New York, NY, USA, 2003.
68. Itam, Z.; Syamsir, A.; Rababah, A.Q.; Malkawi, O.; Razeman, N.A. Utilization of Mango Leaf Ash as a Supplementary Cementitious Material in Concrete. *AIP Conf. Proc.* **2023**, *2544*, 826–841. [CrossRef]
69. Maharishi, A.; Singh, S.P.; Gupta, L.K. Shehnazdeep Strength and Durability Studies on Slag Cement Concrete Made with Copper Slag as Fine Aggregates. *Mater. Today Proc.* **2020**, *38*, 2639–2648. [CrossRef]
70. Danish, A.; Mosaberpanah, M.A. A Review on Recycled Concrete Aggregates (RCA) Characteristics to Promote RCA Utilization in Developing Sustainable Recycled Aggregate Concrete (RAC). *Eur. J. Environ. Civ. Eng.* **2022**, *26*, 6505–6539. [CrossRef]
71. Shaikh, F.U.A. Mechanical Properties of Recycled Aggregate Concrete Containing Ternary Blended Cementitious Materials. *Int. J. Sustain. Built Environ.* **2017**, *6*, 536–543. [CrossRef]
72. Thomas, J.; Thaickavil, N.N.; Wilson, P.M. Strength and Durability of Concrete Containing Recycled Concrete Aggregates. *J. Build. Eng.* **2018**, *19*, 349–365. [CrossRef]
73. Miraldo, S.; Lopes, S.; Pacheco-torgal, F.; Lopes, A. Advantages and Shortcomings of the Utilization of Recycled Wastes as Aggregates in Structural Concretes. *Constr. Build. Mater.* **2021**, *298*, 123729. [CrossRef]
74. Megharani; Thejaswi, K.P.; Prakash, D. Performance of Frc With Partial Replacement of Natural Coarse Aggregate By Recycled Coarse Aggregate, Cement By Fly Ash and Natural Sand By Quarry Dust. *Int. Res. J. Eng. Technol.* **2008**, *6*, 559–564.
75. Qian, R.; Lin, W.W.; Yang, C.; Zhao, R.; Ye, Z.; Kong, D.; Zhang, Y. Investigations on Carbon-Sequestration Optimization of Recycled Coarse-Aggregate and Its Effects on Concrete Performances. *J. Build. Eng.* **2024**, *90*, 109453. [CrossRef]
76. Ouyang, K.; Liu, J.; Liu, S.; Song, B.; Guo, H.; Li, G.; Shi, C. Influence of Pre-Treatment Methods for Recycled Concrete Aggregate on the Performance of Recycled Concrete: A Review. *Resour. Conserv. Recycl.* **2023**, *188*, 106717. [CrossRef]
77. Francioso, V.; Moro, C.; Velay-Lizancos, M. Effect of Recycled Concrete Aggregate (RCA) on Mortar's Thermal Conductivity Susceptibility to Variations of Moisture Content and Ambient Temperature. *J. Build. Eng.* **2021**, *43*, 103208. [CrossRef]
78. Alharthai, M.; Ali, T.; Qureshi, M.Z.; Ahmed, H. The Enhancement of Engineering Characteristics in Recycled Aggregates Concrete Combined Effect of Fly Ash, Silica Fume and PP Fiber. *Alex. Eng. J.* **2024**, *95*, 363–375. [CrossRef]
79. Kapoor, K.; Singh, S.P.; Singh, B. Durability of Self-Compacting Concrete Made with Recycled Concrete Aggregates and Mineral Admixtures. *Constr. Build. Mater.* **2016**, *128*, 67–76. [CrossRef]
80. Wang, Y.; Xiao, R.; Lu, H.; Hu, W.; Jiang, X.; Huang, B. Effect of Curing Conditions on the Strength and Durability of Air Entrained Concrete with and without Fly Ash. *Clean. Mater.* **2023**, *7*, 100170. [CrossRef]
81. Haque, M.I.; Khan, R.I.; Ashraf, W.; Pendse, H. Production of Sustainable, Low-Permeable and Self-Sensing Cementitious Composites Using Biochar. *Sustain. Mater. Technol.* **2021**, *28*, e00279. [CrossRef]
82. Hakeem, I.Y.; Alharthai, M.; Amin, M.; Zeyad, A.M.; Tayeh, B.A.; Agwa, I.S. Properties of Sustainable High-Strength Concrete Containing Large Quantities of Industrial Wastes, Nanosilica and Recycled Aggregates. *J. Mater. Res. Technol.* **2023**, *24*, 7444–7461. [CrossRef]
83. Shi, C.; Zhao, R.; Wang, X.; Wang, W.; Ding, K. Effect of Clay Content on Concrete Properties. *Case Stud. Constr. Mater.* **2024**, *20*, e03341. [CrossRef]
84. Wijayasundara, M.; Crawford, R.H.; Mendis, P. Comparative Assessment of Embodied Energy of Recycled Aggregate Concrete. *J. Clean. Prod.* **2017**, *152*, 406–419. [CrossRef]
85. Bompa, D.V.; Silva, L.F.O.; Saba, M. Geoscience Frontiers Comparative Carbon Emission Assessments of Recycled and Natural Aggregate Concrete: Environmental Influence of Cement Content. *Geosci. Front.* **2021**, *12*, 101235.
86. Fraj, A.B.; Idir, R. Concrete Based on Recycled Aggregates—Recycling and Environmental Analysis: A Case Study of Paris' Region. *Constr. Build. Mater.* **2017**, *157*, 952–964. [CrossRef]
87. Xing, W.; Tam, V.W.Y.; Le, K.N.; Butera, A.; Hao, J.L.; Wang, J. Effects of Mix Design and Functional Unit on Life Cycle Assessment of Recycled Aggregate Concrete: Evidence from CO_2 Concrete. *Constr. Build. Mater.* **2022**, *348*, 128712. [CrossRef]
88. Robayo-Salazar, R.; Mejía-Arcila, J.; Mejía de Gutiérrez, R.; Martínez, E. Life Cycle Assessment (LCA) of an Alkali-Activated Binary Concrete Based on Natural Volcanic Pozzolan: A Comparative Analysis to OPC Concrete. *Constr. Build. Mater.* **2018**, *176*, 103–111. [CrossRef]
89. Dacić, A.; Mester-Szabó, E.; Fenyvesi, O.; Szalay, Z. Life Cycle Assessment of Concrete Incorporating All Concrete Recycling Products. *Case Stud. Constr. Mater.* **2024**, *21*, e03910. [CrossRef]

90. Scrivener, K.L.; John, V.M.; Gartner, E.M. Eco-Efficient Cements: Potential Economically Viable Solutions for a Low-CO_2 Cement-Based Materials Industry. *Cem. Concr. Res.* **2018**, *114*, 2–26. [CrossRef]
91. Akbarnezhad, A.; Xiao, J. Estimation and Minimization of Embodied Carbon of Buildings: A Review. *Buildings* **2017**, *7*, 5. [CrossRef]
92. Xia, B.; Ding, T.; Xiao, J. Life Cycle Assessment of Concrete Structures with Reuse and Recycling Strategies: A Novel Framework and Case Study. *Waste Manag.* **2020**, *105*, 268–278. [CrossRef]

Disclaimer/Publisher's Note: The statements, opinions and data contained in all publications are solely those of the individual author(s) and contributor(s) and not of MDPI and/or the editor(s). MDPI and/or the editor(s) disclaim responsibility for any injury to people or property resulting from any ideas, methods, instructions or products referred to in the content.